

Spin-fluctuation dominated electrical transport of Ni₃Al at high pressure

P. G. Niklowitz,* F. Beckers, and G. G. Lonzarich

Cavendish Laboratory, University of Cambridge, Madingley Road, Cambridge CB3 0HE, UK

G. Knebel, B. Salce, J. Thomasson, N. Bernhoeft, D. Braithwaite, and J. Flouquet

*Département de Recherche Fondamentale sur la Matière Condensée,
SPSMS,CEA Grenoble, 38054 Grenoble Cedex 9, France*

(Dated: December 6, 2018)

We present the first study of a magnetic quantum phase transition in the itinerant-electron ferromagnet Ni₃Al at high pressures. Electrical resistivity measurements in a diamond anvil cell at hydrostatic pressures up to 100 kbar and temperatures as low as 50 mK indicate that the Curie temperature collapses towards absolute zero at a critical pressure $p_c = 82 \pm 2$ kbar. Over wide ranges in pressure and temperature, both in the ferromagnetic and paramagnetic states, the temperature variation of the resistivity is found to deviate from the conventional Fermi-liquid form. We consider the extent to which this deviation can be understood in terms of a mean-field model of enhanced spin fluctuations on the border of ferromagnetism in three dimensions.

PACS numbers: 71.27.+a, 71.10.-w, 75.40.-s, 07.35.+k

Keywords: strongly correlated electrons, weak ferromagnetism, quantum phase transition, spin-fluctuation theory, electrical resistivity, diamond anvil cell, low temperatures

I. INTRODUCTION

The electronic properties of metals on the border of magnetic phase transitions at low temperatures are often found to exhibit temperature dependences at variance with the predictions of the standard model of a normal Fermi liquid. Early attempts to explain such non-Fermi-liquid behaviour have been based on a mean-field treatment of the effects of strongly-enhanced spin-fluctuations (paramagnons).^{1,2,3}

For a metal on the border of ferromagnetism in three spatial dimensions (3D), this mean-field spin-fluctuation model predicts a $T^{5/3}$ temperature dependence of the resistivity,⁴ instead of the conventional T^2 temperature dependence of a normal metal at low temperatures. The $T^{5/3}$ variation of the resistivity is a consequence of an underlying quasiparticle scattering rate that varies linearly with the excitation energy E of a quasiparticle near the Fermi level. This is the behaviour associated not with a Fermi liquid, for which the quasiparticle scattering rate varies as E^2 , but of a cross-over state known as the marginal Fermi liquid.^{5,6,7,8} A review of several underlying models that yield a marginal Fermi-liquid form of the electron self energy is given in Ref. 7.

In contrast to a phenomenological model introduced to describe the normal state of the cuprates,⁵ the marginal Fermi liquid that arises on the border of an itinerant-electron ferromagnet in 3D is due to the scattering of long-wavelength spin fluctuations that are relatively ineffective in reducing the current. This leads to a temperature dependence of the transport relaxation rate or resistivity that is characterized by an exponent above unity, i.e., $5/3$, but still below that expected for a conventional Fermi liquid.⁴

In this paper we re-examine the behaviour of the resistivity on the border of itinerant-electron ferromagnetism

in the relatively simple case of Ni₃Al in which the cross-over from ferromagnetism to paramagnetism is achieved by the application of hydrostatic pressure. Ni₃Al can be prepared in a pure stoichiometric form and crystallizes in a simple cubic (Cu₃Au) structure.⁹ At ambient pressure it orders ferromagnetically below 42 K with a small average moment of $0.075 \mu_B/\text{Ni}$ in the limit of low temperature and low magnetic field.^{10,11,12,13}

For a test of the predictions of the mean-field spin-fluctuation model, Ni₃Al appears to offer advantages over a number of other metals on the border of magnetism. The magnetic critical point can be tuned via hydrostatic pressure as opposed to chemical doping (as in, e.g., Pd(Ni))¹⁴ that can introduce new physics of disorder not incorporated fully in the mean-field spin-fluctuation model. In contrast to other d-metals (e.g., MnSi, CoSi₂),^{15,16,17,18} Ni₃Al has a more nearly continuous quantum phase transition and (unlike MnSi) does not exhibit a spin-spiral structure due to the Moriya-Dzyaloshinski interaction arising from lack of space inversion symmetry. Also, in contrast to the nearly magnetic f-metals (e.g., CeCu_{6-x}Au_x, CePd₂Si₂, YbRh₂Si₂, UGe₂),^{19,20,21,22} the spin-orbit interaction in Ni₃Al is relatively weak, the energy bands are relatively broad and the spin fluctuations are not local in real space, features that may be necessary for the applicability of the mean-field spin-fluctuation model in its present form.

As a reference system for the study of the border of metallic ferromagnetism, Ni₃Al is also convenient because, along with its close relative, the nearly ferromagnetic metal Ni₃Ga, it has been extensively studied using a wide range of experimental techniques,^{23,24,25,26,27,28,29,30,31,32} all of which indicate the importance of spin fluctuations in these materials.^{33,34} The combined results in these two systems define the parameters of the mean-field spin-fluctuation

model that may be relevant to interpreting the behaviour of Ni_3Al from its low-pressure ferromagnetic phase to the high pressure paramagnetic phase near and above p_c where a marginal Fermi liquid cross-over state may be expected to be observed.³⁵

II. EXPERIMENTAL DETAILS

Ni_3Al samples were pressurised using a diamond anvil cell (DAC) described in detail elsewhere.³⁶ The cell employed anvils with culet diameter of 1 mm, a stainless-steel gasket with central hole for the sample and several ruby chips, and Argon as the pressure medium. After compression, the sample space was typically 400 μm in diameter and 50 μm in thickness. The pressure was determined from the fluorescence of the tiny ruby chips in the sample space.³⁷ The noble gas pressure medium ensured that the applied pressure was very hydrostatic. The pressure inhomogeneity over the sample was only 3% of the applied pressure.

The samples were prepared from the melt by radio frequency heating starting with zone refined Ni and Al having residual resistivity ratios of over 2000. High homogeneity samples were obtained by suitable stirring of the high purity stoichiometric melt, followed by rapid quenching and then annealing for up to 6 days. Small single crystals were spark cut from the resulting ingot and then characterised by means of microprobe analysis, transmission electron microscopy, Laue x-ray diffraction, mass spectroscopy, magnetic hysteresis and resistivity ratio measurements. These studies did not reveal evidence of precipitates of other phases or of total metallic impurity levels in excess of 20 ppm. The specimens selected for pressure studies in a ^4He system and in a dilution refrigerator had residual resistivity ratios of 27 and 29, respectively, and had been used previously for the study of the de Haas-van Alphen (dHvA) effect.²⁵ Tiny samples of the size required to fit into the DAC were cut to an initial thickness of 100 μm by means of low-power spark erosion and thinned to the final thickness of 10 μm by chemical polishing.

The resistivity was measured by a sensitive ac 4-terminal technique. Four 12 μm gold wires were attached to the sample by a micro-spot-welding technique that gave low contact resistance and thus low excitation-current heating and high detection sensitivity. Damage to the sample was minimized by spot welding with very low power immediately after the surface of the sample had been cleaned by chemical polishing. The gold wires were passed between one diamond anvil and one side of the stainless steel gasket insulated with a layer of 1266 Stycast epoxy mixed with a saturated concentration of Al_2O_3 powder.³⁸ The resistivity was measured in a ^4He system from 1.5 to 40 K with an excitation current of 1 mA, and in a dilution refrigerator from 50 mK to 6.5 K with an excitation current of 100 mA. The dilution refrigerator contained a low temperature transformer and

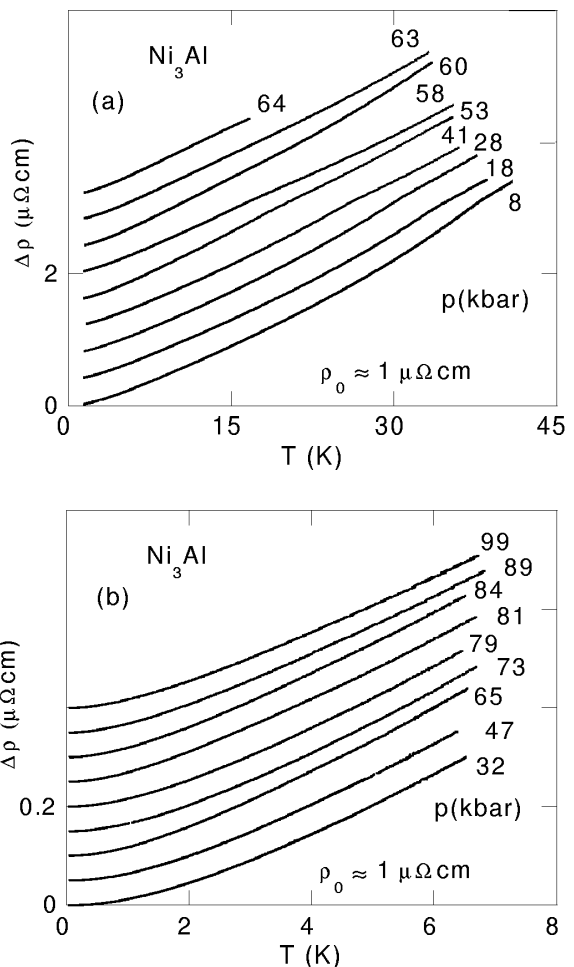


FIG. 1: The temperature-dependent part of the electrical resistivity $\Delta\rho = \rho - \rho_0$ at various pressures. Measurements were carried out in a ^4He system (a) and a dilution refrigerator (b). Upon pressure application ρ_0 increased irreversibly by about $1 \mu\Omega\text{cm}$ and thus the intrinsic pressure dependence of ρ_0 could not be inferred. The curves have been shifted vertically for clarity.

both refrigerators were equipped with a variable force application mechanism that allowed the in-situ changes of the pressure in the DAC.³⁹

III. RESULTS

A. Magnetic phase diagram of Ni_3Al

Our measurements of the temperature dependence of the resistivity of Ni_3Al at different pressures are shown in Figure 1. The temperature dependent part of the resistivity is defined by $\Delta\rho = \rho - \rho_0$, where ρ_0 is the residual resistivity inferred by a suitable extrapolation of ρ vs T to absolute zero of temperature. The small values of ρ_0 , initially of the order of $1 \mu\Omega\text{cm}$ for our sam-

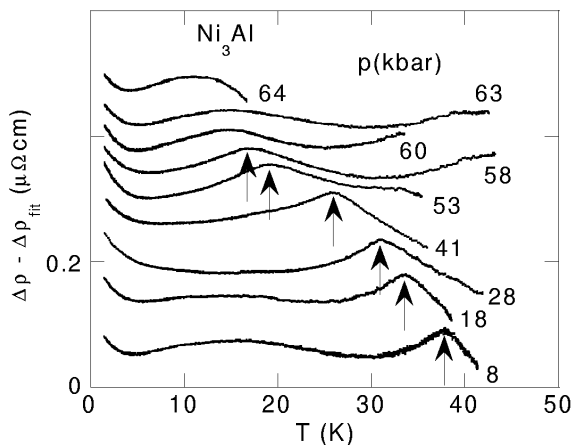


FIG. 2: Signature of the ferromagnetic transition of Ni_3Al in the temperature dependence of the resistivity. The ferromagnetic transition at T_{Curie} indicated by an arrow shows up in a plot of $\Delta\rho - \Delta\rho_{\text{fit}}$ where $\Delta\rho_{\text{fit}}$ is a smooth second-order polynomial fit of the data over the entire experimental range. The same values of T_{Curie} are obtained within experimental error from plots of $\partial\rho/\partial T$ vs T . The curves have been shifted vertically for clarity.

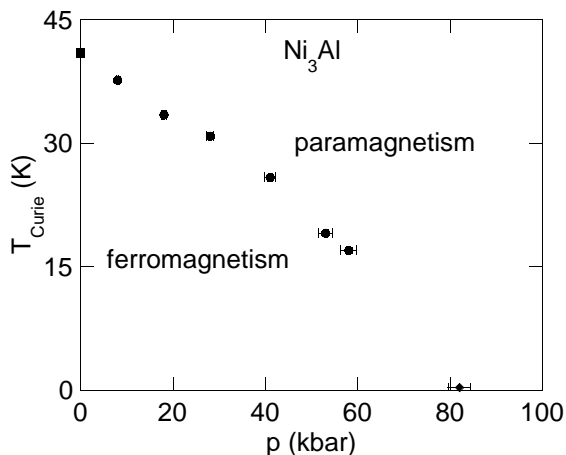


FIG. 3: The proposed magnetic temperature-pressure phase diagram of Ni_3Al . The full circles represent the peaks in the resistivity data $\Delta\rho - \Delta\rho_{\text{fit}}$ in Figure 2. The square represents the ferromagnetic transition $T_{\text{Curie}} = 41 \pm 1$ K at ambient pressures inferred in samples similar to those studied here by means of both resistivity and magnetic susceptibility measurements. The diamond defines the critical pressure $p_c = 82 \pm 2$ kbar inferred from the peak in the T^2 coefficient of the resistivity vs pressure plotted in the inset of Figure 7b.

ples, were found to increase irreversibly by about $1 \mu\Omega\text{cm}$ during the pressure experiments, and thus the intrinsic pressure dependence of ρ_0 could not be inferred. At low and intermediate pressures, the resistivity curves exhibit very weak anomalies in ρ vs T centred at a temperature that coincides at ambient pressure with the Curie temperature T_{Curie} . It is natural to associate the pressure dependence of these anomalies with the pressure de-

pendence of T_{Curie} . The anomalies can be made more evident by plotting the derivative $\partial\rho/\partial T$ or by subtracting from ρ a smooth polynomial fit of the form $\Delta\rho_{\text{fit}} = c_0 + c_1T + c_2T^2$. The curves $\Delta\rho - \Delta\rho_{\text{fit}}$ shown in Figure 2 clearly reveal a peak that collapses monotonically with increasing pressure. Plots of $\partial\rho/\partial T$ and of $\Delta\rho - (c_0 + c_1T)$ also lead to peak positions consistent with those in Figure 2. The weakening of the peaks with increasing pressure is consistent with the predictions of the mean-field spin-fluctuation model. We note that near T_{Curie} the magnetic contribution to $\partial\rho/\partial T$ is quite generally expected to be proportional to the magnetic contribution to the heat capacity,^{40,41} which, in the mean-field spin-fluctuation model, is predicted to decrease with decreasing T_{Curie} .⁴² Particularly at high pressures, however, the peaks may also be reduced by broadening due to pressure inhomogeneities. This effect grows with increasing downward curvature of T_{Curie} vs p and may be expected to lead to a disappearance of the Curie point anomaly in ρ vs T near p_c .

The pressure dependence of T_{Curie} inferred from the resistivity anomalies is shown in Figure 3. T_{Curie} collapses with increasing pressure with an initial gradient of approximately -0.4 ± 0.05 Kkbar⁻¹, which is close to the value reported in an early low-pressure study.⁴³ Assuming a slightly stronger than linear variation, T_{Curie} vs p extrapolates to a value close to $p_c = 82 \pm 2$ kbar defined by the peak in the low-temperature limit of $A = \Delta\rho/T^2$ vs p (see Figure 7). However, the lack of evidence of a clear signature of T_{Curie} in $\Delta\rho$ vs T above 60 kbar leaves some doubt as to the true value of the critical pressure at which T_{Curie} vanishes.

We note that ferromagnetism in Ni_3Al can also be suppressed by Al doping.^{11,44} However, the high sensitivity of T_{Curie} to dopant concentration x in $\text{Ni}_{75-x}\text{Al}_{25+x}$ has made it difficult to produce a detailed temperature-dopant phase diagram for comparison with our temperature-pressure phase diagram. In previous work x was varied in steps of 0.5, corresponding to steps of the order of 100 kbar, and the critical value of x where T_{Curie} vanishes is estimated by interpolation of the data to be about 0.4. Doped specimens have higher ρ_0 and thus lower values of $\Delta\rho/\rho_0$, making measurements of the temperature dependence of ρ more difficult. Also, doped samples may have significant inhomogeneities in T_{Curie} and may involve physics not included in the mean-field spin-fluctuation model.

B. Temperature dependence of the resistivity

The evolution with pressure of the temperature dependence of the resistivity is shown in Figures 4 and 5. The resistivity is plotted against T , $T^{3/2}$, $T^{5/3}$, and T^2 for three pressures corresponding to the lower and upper end of the pressure range of the data in Figure 1b as well as the critical pressure.

Overall the temperature dependent part of the resistiv-

ity appears to be only weakly pressure dependent over the entire pressure range investigated up to nearly 100 kbar. This is in marked contrast to the behaviour of MnSi and, in particular, of narrow f-band materials that in general exhibit obvious and strong variations of the resistivity upon crossing the critical pressure over a pressure range of typically only a few kbar. Ni₃Al differs in its low-temperature resistivity from typical f-band systems in being essentially very near a magnetic quantum critical point over a wide pressure range.

Figures 4 and 5 also show that even at low temperatures, 0.05 K to 7 K, the resistivity cannot be described in terms of a simple power law. The overall best fit in this temperature range is to an exponent of the order of 3/2. Below 4 K, however, the best fit is to an exponent of the order of 5/3 and below 1 K to an exponent of about 2. This behaviour is highlighted in the temperature variation of the logarithmic derivative of the resistivity $\partial \ln \Delta\rho / \partial \ln T$ shown in Figure 6, which defines the temperature dependent resistivity exponent $n(T)$. At still higher temperatures (well above 10 K), the resistivity exponent eventually drops towards unity (see Figure 1a).

For low pressures where comparisons can be made our findings are generally consistent with previous resistivity measurements in stoichiometric samples^{10,12,23,44,45} and in samples in which the ratio of the Ni and Al concentrations were varied so as to suppress ferromagnetic order.²³ In all cases the temperature dependence of the resistivity is found to deviate from the Fermi liquid form and to be described in first approximation in terms of a resistivity exponent around 3/2 in the temperature range 1-30 K. However, in contrast to the present work, these earlier studies did not yield clear evidence for a limiting T^2 form of the resistivity at very low temperatures below 1 K. In particular, Fluitman et al., found a resistivity exponent of the order of 3/2 down to 200 mK in samples with Ni to Al ratios tuned to the critical value where T_{Curie} vanishes.⁴⁶ Furthermore, in a study of several stoichiometric Ni₃Al samples, Steiner et al., found that while above 1 K the resistivity exponent is sample independent, and consistent with our work, below 1 K it varied significantly from sample to sample, exhibiting in some cases weak upturns or downturns below a few hundred mK.⁴⁵

We note that in all samples investigated thus far $\Delta\rho$ is very small compared with ρ_0 at dilution refrigerator temperatures (i.e., $\Delta\rho/\rho_0 < 2\%$ for $T < 1$ K). Thus, the behaviour of $\Delta\rho$ in this range may be sensitive to sample heterogeneities and the precise way by which the samples are prepared. Thus, the form of the resistivity that we observe below 1 K (Figure 7) is not necessarily the property of the ideal stoichiometric state of Ni₃Al. It is interesting to note, however, that the T^2 coefficient A of $\Delta\rho$ in the mK range shows a peak (the peak position we define to be p_c ; inset of Figure 7b). Plots of $\Delta\rho/T^2$ vs T at different pressures in Figure 8 show that the effect of pressure and the approach of a quantum critical point near p_c become most clearly evident in the low

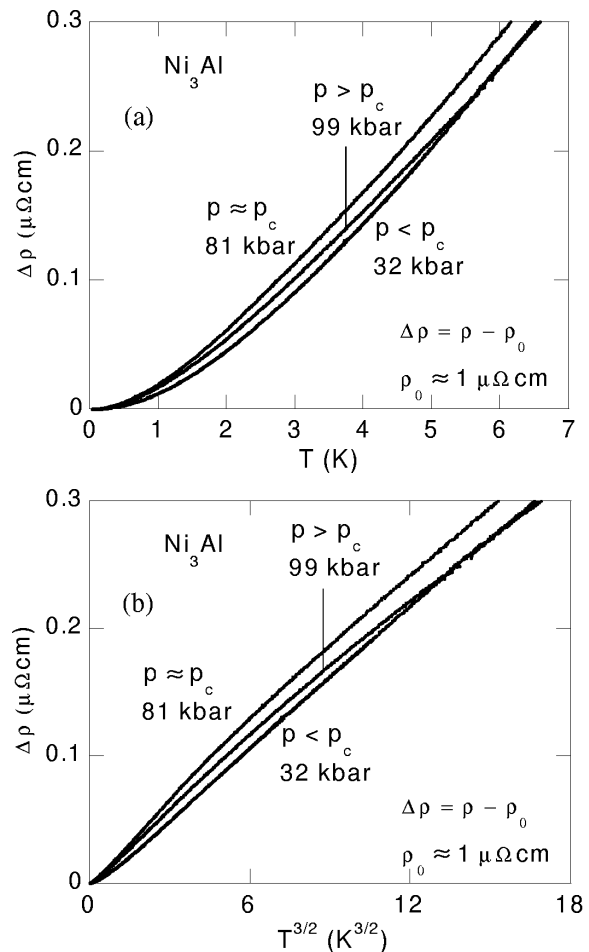


FIG. 4: Temperature-dependent part of the resistivity $\Delta\rho$ of Ni₃Al versus T (a) and versus $T^{3/2}$ (b). $\Delta\rho$ varies more strongly than linear with temperature. At low temperatures, $\Delta\rho$ rises more strongly than $T^{3/2}$ and at higher temperatures $\Delta\rho$ rises more weakly than $T^{3/2}$. As shown in Figure 6 the resistivity exponent, defined by the logarithmic derivative of $\Delta\rho$, is not constant and varies strongly with temperature even in the liquid helium temperature range.

temperature limit. We see that not only is the maximum of $\Delta\rho/T^2$ vs T at p_c strongest at low temperatures but also the crossover temperature above which ρ clearly deviates from the Fermi-liquid form (e.g., the temperature where $\Delta\rho/T^2$ falls by 20% of its value in the zero temperature limit) reaches a minimum at this same pressure. At 81 kbar $\Delta\rho/T^2$ vs T continues to grow with decreasing temperature down to at least below 600 mK where $\Delta\rho \ll \rho_0$ and a well-defined finite value of $A = \Delta\rho/T^2$ as given in the inset of Figure 7b is obtained only after averaging over 500 mK. Although Fluitman et al. did not report observing a T^2 form of $\Delta\rho$, they nevertheless considered the behaviour of the average value between 1.2 and 4.2 K of the ratio $\Delta\rho/T^2$.²³ They find that this ratio varied by a factor of about 1.3 in going from a stoichiometric Ni₃Al sample to a non-stoichiometric sample

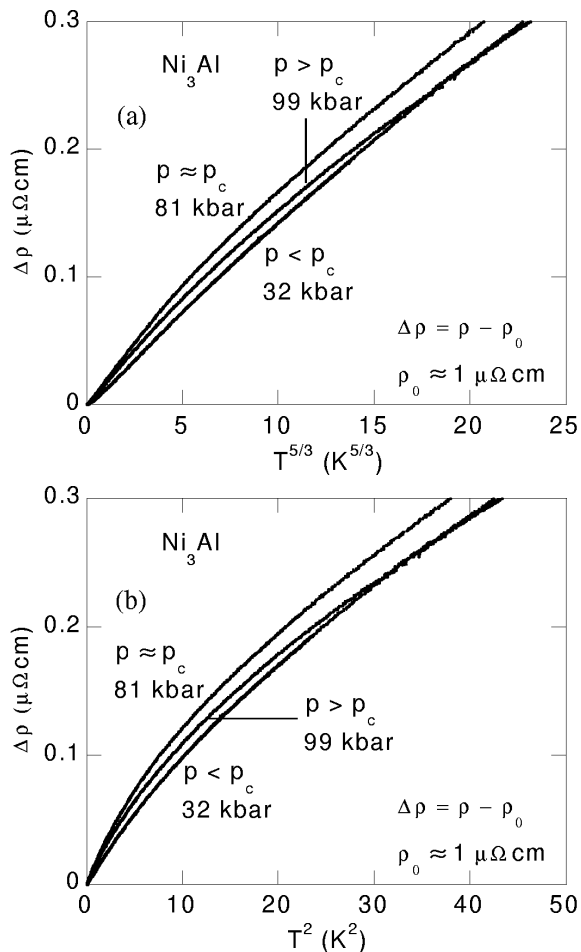


FIG. 5: Temperature-dependent part of the resistivity $\Delta\rho$ of Ni_3Al versus $T^{5/3}$ (a) and versus T^2 (b). The resistivity exponent defined by the logarithmic derivative of $\Delta\rho$ is not constant and increases with decreasing temperature from about 1.5 at 5 K towards 2 below 1 K (Figure 6).

with critical doping where T_{Curie} vanishes. This agrees well with the variation versus pressure of $\Delta\rho/T^2$ in the same temperature range (Figure 8).

IV. DISCUSSION

In the following we discuss our experimental results in terms of an elementary form of the mean-field spin-fluctuation model discussed in the introduction.⁴⁷ Near the critical pressure where ferromagnetic order in 3D vanishes, this model leads to an electron self energy of a form at low energy characteristic of a marginal Fermi liquid.⁴⁸

We consider a 3D isotropic itinerant-electron system in which the total spin is conserved and only long wavelength fluctuations of the magnetization are strongly enhanced by an exchange molecular field arising from the effects of the Coulomb interaction and the Pauli princi-

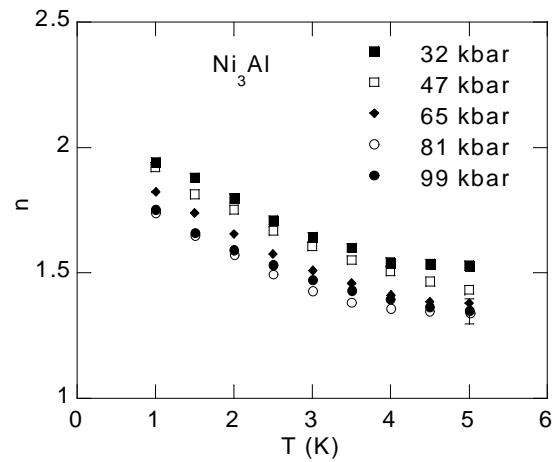


FIG. 6: The resistivity exponent of Ni_3Al defined by the logarithmic derivative of the resistivity, $n = \partial \ln \Delta\rho / \partial \ln T$. The resistivity exponent rises with decreasing temperature from about 1.5 at 5 K towards 2 below 1 K. At each T the exponent is a minimum at around p_c . We note that there is no extended temperature regime for either a T^2 or $T^{5/3}$ behaviour. The error bar given at 5 K applies to all data points shown in the plot.

ple. These conditions may be approximately satisfied in the case of Ni_3Al for the reasons given in the introduction. The essential features of the model are as follows. We assume that in the low T limit the magnetization $\mathbf{M}(\mathbf{r})$ in a weak applied magnetic field $\mathbf{H}(\mathbf{r})$ is given by a Ginzburg-Landau equation of the form

$$\mathbf{H} = a\mathbf{M} + b\mathbf{M}^3 - c\nabla^2\mathbf{M} \quad (1)$$

where $\mathbf{M}^3 = (\mathbf{M} \cdot \mathbf{M})\mathbf{M}$ and b and c are positive constants. The latter conditions imply that the system undergoes a continuous ferromagnetic transition when a crosses zero. As in the Landau mean-field model we assume a is linear in $(p - p_c)$ for p close to the critical pressure p_c , i.e., that $a = \alpha(p - p_c)$, where α is a positive constant. An analytic expansion of a and the mean-field analysis given below is thought to be plausible because the effective dimension relevant to quantum phenomena in the $T \rightarrow 0$ limit is greater than the upper critical dimension in Ni_3Al .^{1,2,3} We also assume that relaxation of a fluctuation of the magnetization $\mathbf{M}(\mathbf{r}, t)$ to equilibrium is governed by Landau damping. Thus, a Fourier component $\mathbf{M}_{\mathbf{q}}(t)$ of $\mathbf{M}(\mathbf{r}, t)$ decays exponentially to the value given by Equation 1 via a relaxation function that is proportional to $q = |\mathbf{q}|$. In zero applied field and small $\mathbf{M}_{\mathbf{q}}$ in the paramagnetic state this implies

$$\frac{\partial \mathbf{M}_{\mathbf{q}}}{\partial t} = -\gamma q(a + cq^2)\mathbf{M}_{\mathbf{q}} \quad (2)$$

where γ is a positive constant. We note that the coefficient of $(-\mathbf{M}_{\mathbf{q}})$ on the right hand side of Equation 2 defines the \mathbf{q} dependent relaxation rate $\Gamma_{\mathbf{q}}$ of magnetic fluctuations. Thus, $\Gamma_{\mathbf{q}}$ is given by γq times the inverse

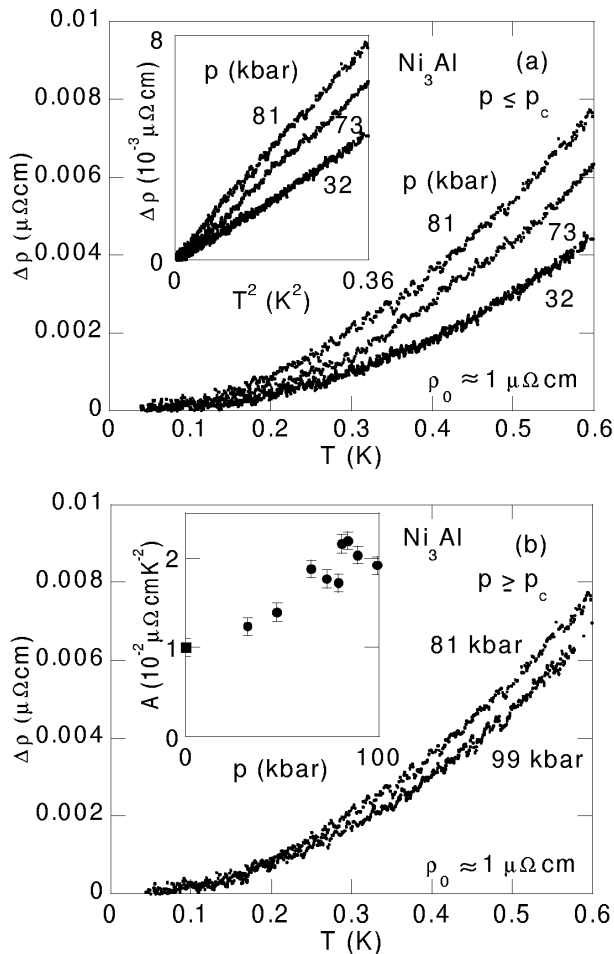


FIG. 7: Temperature dependent part of the resistivity $\Delta\rho$ of Ni_3Al in the millikelvin range. In this range where $\Delta\rho$ is only of the order of 1-2% of ρ_0 , $\Delta\rho$ is approximately of the form AT^2 for our sample. The T^2 coefficient A increases with rising pressure up to $p_c = 82 \pm 2$ kbar (a) and falls again beyond p_c (b). As shown in the inset of Figure (b) the peaks value of A at p_c is a factor of 2 higher than the zero-pressure value of $0.01 \mu\Omega\text{cmK}^{-2}$.¹² A has been determined from a fit of $\Delta\rho$ vs T^2 in the range 50 mK to 600 mK.

static susceptibility, which is defined as the linear coefficient of $\mathbf{M}_{\mathbf{q}}$ in the Fourier transform of Equation 1. Note that when $a \rightarrow 0$ the relaxation rate becomes cubic in q , i.e., the dynamical exponent z is here equal to 3. Thus for $D = 3$ the effective dimension $D + z$ relevant to quantum critical phenomena is equal to 6, which is indeed above the upper critical dimension of 4 for our Ginzburg-Landau model.

The model defined by Equations 1 and 2 is found to be consistent with ambient-pressure bulk magnetization measurements¹¹ that yield the parameters a and b and ambient-pressure inelastic neutron scattering measurements⁴⁹ that yield estimates of c and γ in Ni_3Al . The values of these essentially ground state parameters define the starting point of a model for the temperature

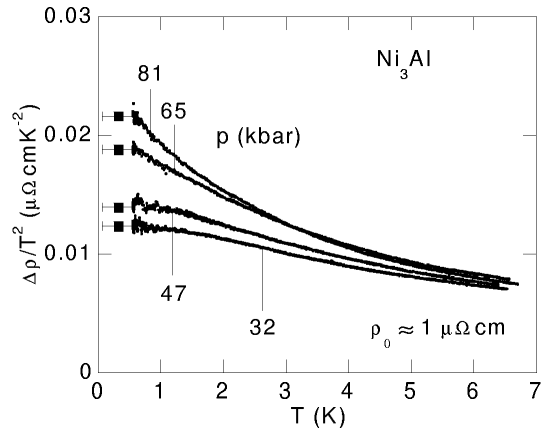


FIG. 8: Pressure dependence of $\Delta\rho/T^2$ versus T in Ni_3Al . The ratio $\Delta\rho/T^2$ increases with decreasing temperature and tends to saturate at low temperature. The characteristic temperature at which saturation occurs decreases with increasing pressure up to the critical pressure ($p_c = 82 \pm 2$ kbar). Correspondingly, the saturation value of $\Delta\rho/T^2$ increases with pressure and peaks near p_c (see inset of Figure 7b). We note that near p_c the saturation of $\Delta\rho/T^2$ is not evident except when averaging over the data from 50 to 600 mK (squares) where $\Delta\rho \ll \rho_0$.

dependence of the magnetic equation of state, heat capacity and resistivity.

The temperature dependence of the magnetic equation of state is assumed to arise primarily from the effects of strongly enhanced long-wavelength spin fluctuations rather than from incoherent particle-hole excitations of conventional band theory. Specifically, any temperature dependence is assumed to arise in a self-consistent way from Equations 1 and 2 together with the Bose function n_ω , which governs the excitations of those spin fluctuations that are strongly excited on the border of magnetic long-range order. Thus, the finite temperature properties are consequences of a set of $T = 0$ parameters and a universal thermal factor in analogy to the Debye model for lattice vibrations or the Fermi liquid model for the quasiparticle excitations of a normal metal at low temperatures. The principal difference is that in the spin-fluctuation model the relevant modes that are thermally excited are not normal modes in the usual sense, but are characterized by a relaxation spectrum (see Equation 2). The self-consistent spin-fluctuation model and the earlier non-self-consistent paramagnon model can thus be viewed as being elementary examples involving the statistical mechanics of open or dissipative systems.^{50,51,52}

A. Magnetic phase boundary

We consider first the effect of thermal fluctuations of the magnetization on the magnetic equation of state (Equation 1). These fluctuations may be imagined to

arise from the effect of a random field of zero mean added to the left hand side of Equation 1 which then drives a random magnetization of zero mean added to the average magnetization in each term on the right hand side of Equation 1. In the absence of the non-linear term on the right hand side of Equation 1 such fluctuations when averaged over an ensemble yield no effect. However, the non-linear term ($b\mathbf{M}^3$) leads to corrections that depend on the variance of the local magnetization. In lowest order, in the paramagnetic state, for example, one finds that the linear coefficient in Equation 1, which represents the inverse uniform susceptibility, becomes

$$a \rightarrow \alpha(p - p_c) + \frac{5}{3}b \langle |\mathbf{m}|^2 \rangle \quad (3)$$

$$\langle |\mathbf{m}|^2 \rangle = \sum_{\mathbf{q}} \langle |\mathbf{m}_{\mathbf{q}}|^2 \rangle \quad (4)$$

$$\langle |\mathbf{m}_{\mathbf{q}}|^2 \rangle = \frac{2}{\pi} \int_0^\infty d\omega (n_\omega) \text{Im} \chi_{\mathbf{q}\omega} \quad (5)$$

where $\langle |\mathbf{m}_{\mathbf{q}}|^2 \rangle$ is the thermal variance of a Fourier component of the fluctuating component of the magnetization and the sum is per unit of volume. The thermal variance $\langle |\mathbf{m}_{\mathbf{q}}|^2 \rangle$ is defined by the fluctuation-dissipation theorem in terms of n_ω and the wavevector and frequency dependent susceptibility $\chi_{\mathbf{q}\omega}$. In our model the latter is given by Equations 1 and 2, but with a replaced as in Equation 3. This yields a self-consistent equation for $\langle |\mathbf{m}_{\mathbf{q}}|^2 \rangle$ and thus the magnetic equation of state versus temperature and pressure. (Note that the zero-point contribution to the total variance of the local magnetization is not included in Equation 5. For further discussions see, e.g., Refs. 31 and 43.)

The Curie temperature is defined by a vanishing linear coefficient in the magnetic equation of state. Equations 1-5 then yield under our assumption and for $p < p_c$,

$$T_{Curie} \approx 2.39c\gamma^{\frac{1}{4}} \left(\frac{\alpha(p_c - p)}{b} \right)^{\frac{3}{4}} \quad (6)$$

Therefore, near p_c , the Curie temperature should vary as $(p_c - p)^{3/4}$ and depend solely on the ground state parameters of the model defined by Equations 1 and 2. This result holds only for sufficiently low values of T_{Curie} where the breakdown region of the mean-field approximation around T_{Curie} is sufficiently narrow. From the measured parameters Equation 6 yields a value of T_{Curie} of the order of 40 K for Ni₃Al at ambient pressure, in good agreement with experiment.³⁵ Our observed pressure dependence of T_{Curie} is not inconsistent with the model, although more detailed measurements near p_c are needed to provide a test of the predicted $(p_c - p)^{3/4}$ variation of T_{Curie} . The phenomenological parameters in

the model might be inferred from an appropriate energy-band model that includes effects of zero-point spin fluctuations. Recently, such a model has been considered and it leads in particular to insights into the origin of the pressure dependence of the ordered moment in Ni₃Al.^{33,34}

B. Temperature dependence of the resistivity

Next we consider the effect of thermal spin fluctuations on the resistivity. Within the Boltzmann-Born model⁵³ one finds that $\Delta\rho$ in the paramagnetic state can be expressed in the form

$$\Delta\rho = \eta \sum_{\mathbf{q}} q \left(T \frac{\partial \langle |\mathbf{m}_{\mathbf{q}}|^2 \rangle}{\partial T} \right)_{\Gamma_{\mathbf{q}}} \quad (7)$$

where η is a constant. The temperature derivative is solely with respect to the Bose function entering the definition of the thermal variance. We have assumed that momentum is efficiently transferred from spin fluctuation to the lattice either by Umklapp processes or residual disorder. The thermal variance of the local magnetisation arises in Equation 7 because current carriers are assumed to undergo weak scattering from a molecular exchange field that is proportional to the local magnetization. Multiple scattering processes are not included. The factor q in Equation 7 comes from a product of (i) a q^2 factor arising from the fact that low q fluctuations are ineffective in reducing the current and (ii) a partly compensating $1/q$ factor due to a loss of wavevector phase space coming from the Pauli principle that constrains scattering to the vicinity of the Fermi surface. Corrections due to momentum non-conservation possibly arising from residual disorder or intraband transitions are not included. The temperature derivative $T\partial/\partial T$ can be shown to arise essentially from the fact that the available momentum phase space increases with increasing temperature due to the thermal depopulation of states below the Fermi surface.

Below a characteristic temperature T_{FL} the above model (Equations 1-7) leads to $\Delta\rho$ of the form $\Delta\rho = AT^2$ where A is inversely related to the square of the temperature T_{FL} that vanishes as $p \rightarrow p_c$. At this pressure $\Delta\rho$ is predicted to vary as $T^{5/3}$ in the low T limit. An elementary discussion of (i) the connection of T_{FL} to the model parameters and (ii) the $T^{5/3}$ form of the resistivity and its connection to the marginal Fermi liquid model may be found for example in Ref. 15.

An extension of the above treatment into the ferromagnetic state^{3,35} leads again to a T^2 resistivity below a characteristic temperature T_{FL} and a $T^{5/3}$ resistivity above T_{Curie} , but below another characteristic temperature T_{MFL} . Above T_{MFL} the resistivity exponent decreases and tends to unity at higher T due to the growth of the thermal variance of the local magnetization in Equation 3, i.e., due to the coupling between spin fluctuation modes in the mean field approximation.

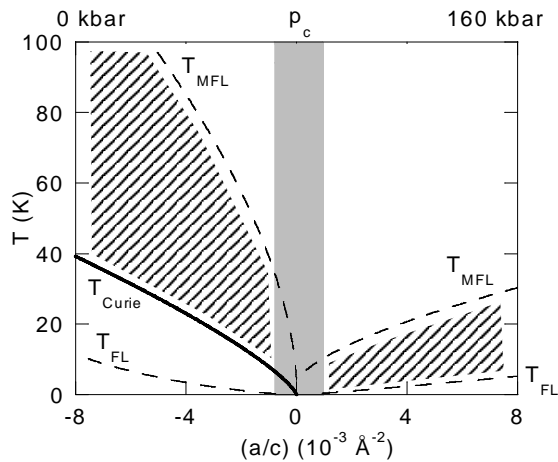


FIG. 9: Temperature-pressure phase diagram predicted by the mean-field spin-fluctuation model discussed in the text. For $p > p_c$ the lower axis represents the square of the magnetic correlation vector (inverse magnetic correlation length) in the zero temperature limit. The solid line represents the Curie temperature given by Equation 6. The crossover lines T_{FL} and T_{MFL} are defined in the text. If the ferromagnetic transition becomes first order at low temperatures, then there exists a region (vertical shading) of forbidden values of a/c .⁵⁴

C. Temperature-pressure phase diagram for Ni₃Al

The above findings are summarized in the predicted temperature-pressure phase diagram for Ni₃Al shown in Figure 9. The pressure dependences of T_{Curie} below p_c and of T_{MFL} and T_{FL} in the paramagnetic state below or above p_c are obtained from (i) Equations 1-7, (ii) the model parameters as defined in Ref. 35, and (iii) $p_c = 82$ kbar. The values of T_{FL} below p_c are obtained by an extension of the model to the ferromagnetic state.^{3,35} The ferromagnetic transition is assumed to be everywhere continuous. The Curie temperature T_{Curie} is defined by Equation 6. The characteristic crossover temperature T_{FL} is defined by the condition $n(T_{FL}) = \ln \Delta \rho / \ln T = 1.8$ and the crossover temperature T_{MFL} by the condition $n(T_{MFL}) = 1.6$.

D. Comparison with experiment

We find that the experimental results may be understood quite well in terms of the above model over a wide range in temperature and pressure, except in the range of about 1-10 K. The regions of agreement and disagreement between the model and experiment are illustrated in the examples shown in Figure 10. The variation of $\Delta \rho$ vs $T^{5/3}$ in two samples of Ni₃Al with different T_{Curie} is plotted in normalized form in Figure 10b.⁵⁵ The predictions of the model for the set of parameters appropriate to the two samples are shown in Figure 10a.³⁵ The agreement between theory and experiment is rather striking both in the magnitudes of T_{Curie} and the overall form of

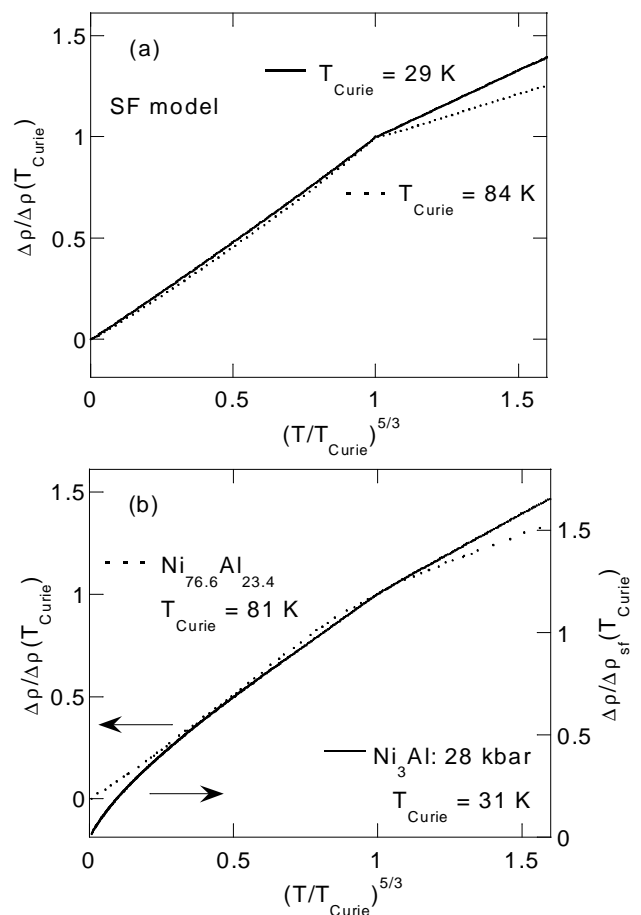


FIG. 10: The temperature dependent part of the resistivity $\Delta \rho$ vs $T^{5/3}$ normalized to values at T_{Curie} . Predictions of the mean-field spin-fluctuation model (a) and experimental findings (b) for two samples with different values of T_{Curie} . The higher value of T_{Curie} was obtained by chemical doping⁵⁵ and the lower value by the application of hydrostatic pressure to our stoichiometric samples (Figure 1a). The correspondence between theory and experiment is strikingly close except for the sample with the lower T_{Curie} at low temperatures. This discrepancy at low T , which indicates an extra component in $\Delta \rho$ additional to the spin-fluctuation component $\Delta \rho_{sf}$, extends up to p_c and beyond. It is also visible in earlier ambient pressure data in a stoichiometric sample.^{12,54,56}

the curves.

However, the stoichiometric sample at high pressure exhibits an anomalous downturn at low T which is not anticipated by the model. This discrepancy is present in all of our high precision measurements in stoichiometric samples up to p_c and beyond. It is also evident in an earlier study at ambient pressure.¹² The above model predicts a $T^{5/3}$ form of $\Delta \rho$ at all T below approximately 10 K at the critical pressure. This is not observed (Figure 6). Instead, as discussed earlier, we observe a continuous change in $x(T)$ varying from approximately 1.3 towards 2 as the temperature is decreased from 5 K to below 1 K.

The T^2 temperature dependence seen away from p_c is qualitatively consistent with the model. However, the magnitude of T_{FL} estimated from Figure 6 or from Figure 8 appears to be nearly an order of magnitude lower than predicted by the model (Figure 9).

E. Corrections to the elementary mean-field spin-fluctuation model

The existence of a T^2 regime at p_c well below 1 K is not expected if the ferromagnetic transition is second order. A finite T_{FL} at p_c may indicate that the phase transition becomes first order close to p_c as might be generally expected for ferromagnetic quantum phase transitions.^{57,58} Here we note that, as found in MnSi, a first order transition need not lead to a Fermi liquid form of $\Delta\rho$ near p_c (i.e., where T_{Curie} vanishes).⁵⁹

The most significant challenge to the mean-field spin-fluctuation model is to account for the anomalous downturn seen in Figure 10b, which was not anticipated and remains unexplained. We stress, however, that in other respects the mean-field spin-fluctuation model provides a rather accurate description of the temperature-pressure phase diagram of Ni₃Al.

The low temperature form of the resistivity is also poorly understood in a number of other materials. In MnSi one observes a $T^{3/2}$ variation of $\Delta\rho$ over nearly 3 decades below 10 K in an extended range in pressure beyond the critical pressure of a first order magnetic transition.^{59,60,61} This is at odds with the prediction that T_{FL} should be of the order of 5 K or higher at all pressures in this system. In ϵ -Fe the resistivity varies as $T^{5/3}$ over two decades above the critical pressure of a first order magnetic and structural phase transition. Naively one would have expect to see a T^2 resistivity below a few K in this system too.^{62,63}

Non-Fermi liquid forms of the resistivity have now been observed in a large number of examples in which the applicability of the mean-field spin-fluctuation model is questionable (see, e.g., Refs 45,64,65). The cases of MnSi and Ni₃Al may stand out partly because the magnitudes of the discrepancies between the predictions and the experimental findings can be quantified in terms of independently determined model parameters. Also, in these two materials the discrepancies arise in small pockets of the temperature-pressure phase diagrams surrounded by wide regions where the mean-field spin-fluctuation model provides a rather accurate description of the experimental findings.

The systems in which the discrepancies between theory and experiment are most clearly evident are characterized by first order transitions for sufficiently low T_{Curie} . This implies that the parameter b in Equation 1 must be taken to be negative, i.e., the coupling between the spin-fluctuation modes is attractive. The applicability in this case of the mean-field decoupling method is not self-evident. Systems described by a quantum Ginzburg-

Landau model in which $b < 0$ (but higher order coefficients in the expansion in M are positive) may be characterized by highly anharmonic magnetic fluctuations not described in the mean-field approximation. Such fluctuations may be of particular interest in cases when the tricritical point characteristic of this extended quantum Ginzburg-Landau model is at sufficiently low temperatures.

Beyond this one may also look for an explanation of the discrepancies between experiment and the mean-field spin-fluctuation model in a number of more conventional effects arising from lattice vibrations,^{10,66} band degeneracies,⁶⁷ Umklapp processes⁶⁸ and quenched disorder. A systematic study of such effects is still lacking for the systems we have considered. We note, however, that the effects of conventional phonon scattering, in particular, is expected to be very weak and ignorable in Ni₃Al at least below 100 K.¹⁰ Also, the effects of quenched disorder may be expected to be strongest below 1 K where $\Delta\rho \ll \rho_0$ in our Ni₃Al samples. However, the behaviour of $\Delta\rho$ vs T in this regime is not inconsistent with our model predictions except perhaps very near p_c . For example, $\Delta\rho/T^2$ at 500 mK is predicted to increase by a factor of about 2 from ambient pressure to p_c . This agrees well with the variation of A shown in the inset of Figure 7b. These considerations suggest that the anomalous behaviour of $\Delta\rho$ in the range 1-10 K may arise from essentially intrinsic effects of the electron-electron interaction and not explicitly from phonons or quenched disorder.

V. CONCLUSION

The magnetic temperature-pressure phase diagram for Ni₃Al has been explored for the first time beyond the low-pressure regime by means of 4 terminal resistivity measurements in a diamond anvil cell. Hydrostatic pressure studies up to 100 kbar and down to 50 mK indicate that the Curie temperature collapses towards absolute zero at a critical pressure $p_c = 82 \pm 2$ kbar.

A non-Fermi liquid form of the resistivity is observed over a wide range in temperature and pressure except below a characteristic temperature T_{FL} that decreases from a few Kelvin at ambient pressure to well below one Kelvin at p_c . The finite value of T_{FL} at p_c may indicate that the ferromagnetic transition is first order near the critical pressure. The temperature dependence of the resistivity and T_{Curie} is, overall, consistent with the predictions of the mean-field spin-fluctuation model, which reduces to a type of marginal Fermi liquid model just above T_{Curie} when T_{Curie} tends towards absolute zero. However, a comparison of theory and experiment also reveals the existence of an extra component in the temperature dependence of the resistivity at intermediate temperatures that has a different and unidentified origin.

Acknowledgments

We wish to thank S. Julian, A. Rosch, A. Huxley and S. Yates for stimulating discussions on this topic. PGN

-
- * e-mail: niklowit@drfmc.ceng.cea.fr; present address: Département de Recherche Fondamentale sur la Matière Condensée, SPSMS, CEA Grenoble, 38054 Grenoble Cedex 9, France
- ¹ J. A. Hertz, Phys.Rev.B **14**, 1165 (1976), and references therein.
 - ² A. J. Millis, Phys.Rev.B **48**, 7183 (1993), and references therein.
 - ³ T. Moriya, *Spin Fluctuations in Itinerant Electron Magnetism* (Springer, Berlin, 1985), and references therein.
 - ⁴ J. Mathon, Proc.Roy.Soc.A **306**, 355 (1968).
 - ⁵ C. M. Varma, P. B. Littlewood, S. Schmitt-Rink, E. Abrahams, and A. E. Ruckenstein, Phys.Rev.Lett. **63**, 1996 (1989).
 - ⁶ T. Holstein, R. E. Norton, and P. Pincus, Phys.Rev.B **8**, 2647 (1973).
 - ⁷ G. Baym and C. Pethick, *Landau-Fermi liquid theory* (Wiley, New York, 1991), chap. 3.
 - ⁸ A relaxation rate linear in E might be expected to give rise to a resistivity varying as T rather than as $T^{5/3}$. The extra factor of $T^{2/3}$ arises in our case because spin-fluctuations or paramagnons on the border of ferromagnetism give rise to scattering mainly in the forward direction and are thus relatively ineffective in reducing the current.
 - ⁹ W. G. Moffatt, *The Handbook of Binary Phase Diagrams* (Genium Publishing Corporation, New York, 1983).
 - ¹⁰ J. H. Fluitman, B. R. de Vries, R. Boom, and C. J. Schinkel, Phys.Lett.A **28**, 506 (1969).
 - ¹¹ F. R. de Boer, C. J. Schinkel, J. Biesterbros, and S. Proost, J.Appl.Phys. **40**, 1049 (1969).
 - ¹² H. Sasakura, K. Suzuki, and Y. Masuda, J.Phys.Soc.Jpn. **53**, 352 (1984).
 - ¹³ N. R. Bernhoeft, Ph.D. thesis, University of Cambridge (1982).
 - ¹⁴ M. Nicklas, M. Brando, G. Knebel, F. Mayr, W. Trinkl, and A. Loidl, Phys.Rev.Lett. **82**, 4268 (1999).
 - ¹⁵ C. Pfeleiderer, G. J. McMullan, S. R. Julian, and G. G. Lonzarich, Phys.Rev.B **55**, 8330 (1997).
 - ¹⁶ C. Thessieu, C. Pfeleiderer, A. N. Stepanov, and J. Flouquet, J.Phys.Cond.Mat. **9**, 6677 (1997).
 - ¹⁷ N. V. Mushnikov and T. Goto, Phys. of Metals and Metallography **93**, S88 (2002).
 - ¹⁸ S. Barakat, Ph.D. thesis, University of Cambridge (2004).
 - ¹⁹ A. Schröder, G. Aeppli, R. Coldea, M. Adams, O. Stockert, H. Löhneisen, E. Bucher, R. Ramazashvili, and P. Coleman, Nature **407**, 351 (2000).
 - ²⁰ J. Custers, P. Gegenwart, H. Wilhelm, K. Neumaier, Y. Tokiwa, O. Trovarelli, C. Geibel, F. Steglich, C. Pepin, and P. Coleman, Nature **424**, 524 (2003).
 - ²¹ S. S. Saxena, P. Agarwal, K. Ahilan, F. M. Grosche, R. K. W. Haselwimmer, M. J. Steiner, E. Pugh, I. R. Walker, S. R. Julian, P. Monthoux, et al., Nature **406**, 587 (2000).
 - ²² N. D. Mathur, F. M. Grosche, S. R. Julian, I. R. Walker, D. M. Freye, R. K. W. Haselwimmer, and G. G. Lonzarich, Nature **394**, 39 (1998).
 - ²³ J. H. J. Fluitman, R. Boom, P. F. de Chatel, C. J. Schinkel, J. L. L. Tilanus, and B. R. de Vries, J.Phys.F **3**, 109 (1973).
 - ²⁴ N. Buis, J. J. Franse, and P. E. Brommer, Physica B **106**, 1 (1981).
 - ²⁵ T. I. Sigfusson, N. R. Bernhoeft, and G. G. Lonzarich, J.Phys.F:Met.Phys. **14**, 2141 (1984).
 - ²⁶ J. J. M. Buiting, J. Kuebler, and F. M. Mueller, J.Phys.F **13**, L179 (1983).
 - ²⁷ N. R. Bernhoeft, G. G. Lonzarich, P. W. Mitchell, and D. M. Paul, Phys.Rev.B **28**, 422 (1983).
 - ²⁸ N. R. Bernhoeft, G. G. Lonzarich, P. W. Mitchell, and D. M. Paul, PhysicaB **136**, 443 (1986).
 - ²⁹ N. R. Bernhoeft, S. M. Hayden, G. G. Lonzarich, D. M. Paul, and E. J. Lindley, Phys.Rev.Lett. **62**, 657 (1989).
 - ³⁰ S. K. Dhar, K. A. Gschneidner, L. L. Miller, and D. C. Johnston, Phys.Rev.B **40**, 11488 (1989).
 - ³¹ F. Semadeni, B. Roessli, P. Böni, P. Vorderwisch, and T. Chatterji, Phys.Rev.B **62**, 1083 (2000).
 - ³² S. H. Kilcoyne and R. Cywinski, PhysicaB **326**, 577 (2003).
 - ³³ A. Aguayo, I. I. Mazin, and D. J. Singh, Phys.Rev.Lett. **92**, 147201 (2004).
 - ³⁴ I. I. Mazin, D. J. Singh, and A. Aguayo, cond-mat/0401563.
 - ³⁵ G. G. Lonzarich and L. Taillefer, J.Phys.C:Solid State Phys. **18**, 4339 (1985).
 - ³⁶ J. Thomasson, F. Thomas, C. Ayache, I. L. Spain, and M. Villedieu, in *Frontiers of High Pressure Research*, edited by H. D. Hochheimer and R. D. Eppers (Plenum, 1991), pp. 423–432.
 - ³⁷ A. Jayaraman, Rev.Mod.Phys. **55**, 65 (1983).
 - ³⁸ J. Thomasson, Y. Okayama, I. Sheikin, J.-P. Brison, and D. Braithwaite, SolidStateComm. **106**, 637 (1998).
 - ³⁹ B. Salce, J. Thomasson, A. Demuer, J. J. Blanchard, J. M. Martinod, L. Devoille, and A. Guillaume, Rev.Sci.Instrum. **71**, 2461 (2000).
 - ⁴⁰ M. E. Fisher and J. S. Langer, Phys.Rev.Lett. **20**, 665 (1968).
 - ⁴¹ S. Alexander, J. S. Helman, and I. Balberg, Phys.Rev.B **13**, 304 (1976).
 - ⁴² K. K. Murata and S. Doniach, Phys.Rev.Lett. **29**, 285 (1972).
 - ⁴³ N. Buis, J. J. M. Franse, J. van Haarst, J. P. J. Kaandorp, and T. Weesing, Phys.Lett. **56**, 115 (1976).
 - ⁴⁴ M. Yoshizawa, H. Seki, K. Ikeda, K. Okuno, M. Saito, and K. Shigematsu, J.Phys.Soc.Jpn **61**, 3313 (1992).
 - ⁴⁵ M. J. Steiner, F. Beckers, P. G. Niklowitz, and G. G. Lonzarich, PhysicaB **329-333**, 1079 (2003).
 - ⁴⁶ J. H. Fluitman, Ph.D. thesis, University of Amsterdam (1970).
 - ⁴⁷ G. G. Lonzarich, *Electron* (Cambridge University Press, Cambridge, 1997), chap. 6.
 - ⁴⁸ I. E. Dzyaloshinskii and P. S. Kondratenko, JETP **43**, 1036 (1976).
 - ⁴⁹ N. R. Bernhoeft, I. Cole, G. G. Lonzarich, and G. L.

- Squires, J.Appl.Phys. **53**, 8204 (1982).
- ⁵⁰ G. G. Lonzarich, J.Magn.Magn.Mat. **54-57**, 612 (1986).
- ⁵¹ A. B. Pippard, Eur.J.Phys. **8**, 55 (1987).
- ⁵² D. M. Edwards and G. G. Lonzarich, Phil.Mag.B **65**, 1185 (1992).
- ⁵³ J. M. Ziman, *Electrons and Phonons* (Clarendon Press, Oxford, 1960).
- ⁵⁴ The parameters of our model for stoichiometric Ni₃Al at ambient pressure are given in Ref. 35. It is assumed that only the critical parameter a varies appreciably with pressure p or doping x . The value of a as a function of p and x is obtained from its value at $p = x = 0$ times $\beta(p, x) = M_0^2(p, x)/M_0^2(0, 0)$, where $M_0(p, x)$ is the magnetization in the zero temperature and zero field limit (see Equation 1). In the analyses presented in this paper, $\beta(0, x)$ is inferred from the data in Ref. 55 and $\beta(p, 0)$ is taken to be $(1 - p/p_c)$ for $p < p_c$ (see Equation 1 and the assumed form of a vs p).
- ⁵⁵ C. J. Fuller, C. L. Lin, T. Mihalisin, F. Chu, and N. Bykovetz, Solid State Commun. **83**, 863 (1992).
- ⁵⁶ The data for the sample with the lower T_{Curie} is only normalised with respect to $\Delta\rho_{sf}(T_{Curie})$. Motivated by the theoretical simulation $\Delta\rho_{sf}(T_{Curie})$ is determined by a $T^{5/3}$ fit to the data from 10 K to T_{Curie} and extrapolation of this fit to $T = 0$ K.
- ⁵⁷ D. Belitz, T. R. Kirkpatrick, and T. Vojta, Phys.Rev.Lett. **82**, 4707 (1999).
- ⁵⁸ A. V. Chubukov, C. Pepin, and J. Rech, Phys.Rev.Lett. **92**, 147003 (2004).
- ⁵⁹ N. Doiron-Leyraud, I. R. Walker, L. Taillefer, M. J. Steiner, S. R. Julian, and G. G. Lonzarich, Nature **425**, 595 (2003).
- ⁶⁰ C. Pleiderer, S. R. Julian, and G. G. Lonzarich, Nature **414**, 427 (2001).
- ⁶¹ C. Pfleiderer, D. Reznik, L. Pintschovius, H. v. Löhneisen, M. Garst, and A. Rosch, Nature **427**, 227 (2004).
- ⁶² D. Jaccard, A. T. Holmes, G. Behr, Y. Inada, and Y. Onuki, Phys.Lett.A **299**, 282 (2002).
- ⁶³ T. Jarlborg, Phys.Lett.A **300**, 518 (2002).
- ⁶⁴ L. Capogna, A. P. Mackenzie, R. S. Perry, S. A. Grigera, L. M. Galvin, P. Raychaudhuri, A. J. Schofield, C. S. Alexander, G. Cao, S. R. Julian, and Y. Maeno, Phys.Rev.Lett. **88**, 76602 (2002).
- ⁶⁵ F. Rivadulla, J.-S. Zhou, and J. B. Goodenough, Phys.Rev.B **67**, 165110 (2003).
- ⁶⁶ C. Stassis, F. X. Kayser, C.-K. Loong, and D. Arch, Phys.Rev.B **24**, 3048 (1981).
- ⁶⁷ G. J. Morgan and J. R. Cooper, J.Phys.F **11**, 2091 (1981).
- ⁶⁸ N. W. Ashcroft and N. D. Mermin, *Solid State Physics* (Saunders College Publishing, Fort Worth, 1976).